inter.noise 2014
MELBOURNE AUSTRALIA
16-19 NOVEMBER

Modelling underwater shipping noise in the Great Barrier Reef Marine Park using AIS vessel track data

Alexander MacGillivray[1], Craig McPherson[2], Geoff McPherson[3], Jonathan Izett[1], Jeremy Gosselin[1], Zizheng Li[1], David Hannay[1]

[1] JASCO Applied Sciences (Canada) Ltd., Canada

[2] JASCO Applied Sciences (Australia) Pty Ltd., Australia

[3] James Cook University, School of Engineering and Physical Sciences, Australia

ABSTRACT

Shipping traffic is the largest contributor of anthropogenic noise in the ocean. Chronic exposure to shipping noise may be a significant habitat-level stressor to marine fauna. While sound measurements can characterise shipping noise at discrete locations and depths, acoustic models can predict anthropogenic sound levels over large regions of the ocean provided the types and locations of all important sound sources are known. We have developed one such model that uses Automated Identification System (AIS) ship tracking data and wind speed data to simulate the time-dependent noise field originating from many ships inside a large number of ships over a wide geographic area. We apply this model to simulate noise from ship traffic in a 25,000 km² region of the Great Barrier Reef Marine Park, off the coast of Townsville, Qld, using three months of AIS data. Acoustic source levels are assigned to the vessels present based on the respective ship-class information embedded in the AIS records. Frequency-dependent propagation loss functions in four dimensions (three spatial and time) are pre-computed for several zones within the study area, based on local bathymetry, geoacoustic, and water column properties. Modelled shipping noise predictions are compared with acoustic measurements collected at Wheeler Reef, off Townsville from April–July 2013.

Keywords: Underwater noise, ambient noise, shipping, Great Barrier Reef, computational acoustics

1. INTRODUCTION

Over the past year, concern regarding environmental effects caused by shipping near the Great Barrier Reef Marine Park (GBRMP) has increased, due in part to the Australian Maritime Safety Authority (AMSA) developing the North-East Shipping Management Plan (1), and the Great Barrier Reef Marine Park Authority (GBRMPA) issuing a Ports and Shipping Information Sheet. The latter acknowledges a possibility of "increased underwater noise resulting in displacement, hearing loss and stranding" (2) of marine mammals. This increased interest prompted JASCO Applied Sciences to initiate a collaborative effort with James Cook University's (JCU) Centre for Sustainable Tropical Fisheries and Aquaculture (CSTFA) to conduct a three month acoustic recording program to characterise the baseline acoustic environment, including shipping noise, at Wheeler Reef, off the coast of Townsville, Qld.

Hydrophone recordings can characterise the marine soundscape well at discrete locations of interest but are less capable of characterising spatial variations unless very many sensors are deployed. An efficient alternative to assess underwater noise over large spatial and temporal scales is to use computational acoustic models. When provided with adequate input data, models can accurately estimate instantaneous and cumulative noise from a large number of sources over wide geographic areas.

JASCO has been developing advanced computational methods that allow multiple moving sources to be modelled simultaneously over a wide area. These methods combine frequency-dependent source levels for different classes of vessels with spatially-varying estimates of transmission loss based on local

[1] alex.macgillivray@jasco.com
[2] craig.mcpherson@jasco.com
[3] geoff.mcpherson@jcu.edu.au

environmental properties. The research discussed in this paper applies these methods to the novel environment of the GBRMP, with vessel movements based on three months of shore-based AIS ship tracking data. The accuracy of these methods is assessed by comparing modelled shipping noise levels to the acoustic data collected at Wheeler Reef.

2. METHODS

2.1 Acoustic Data Collection and Processing

JASCO provided an Autonomous Multichannel Acoustic Recorder (AMAR) to JCU's CSTFA for deployment at Wheeler Reef. The AMAR was configured with a calibrated Geospectrum M8E omnidirectional reference hydrophone (GeoSpectrum Technologies Inc., −165 ± 5 dB re 1 V/µPa nominal sensitivity). Data were recorded on a 24-bit channel sampling at 64 kHz, with an effective bandwidth of 2 Hz to 32 kHz, and a 16-bit channel sampling at 375 kHz, with an effective bandwidth of 8–180 kHz. Both channels were set to 0 dB gain. The recorder has an equivalent spectral noise floor of 23 dB re 1 μPa^2/Hz at 48 kHz and a broadband saturation level of 171 dB re 1 µPa. The AMAR was configured to sample according to the following duty cycle: 428 seconds at 64 kHz, 131 seconds at 375 kHz, and 341 seconds sleep. CSTFA used a team of professional research divers to deploy the AMAR on 24 Apr 2013 at 18.80349° S, 147.52422° E in 14.5 m of water. The same CSTFA team retrieved the AMAR on 29 Jul 2013.

We only used the 64 kHz data to compare with the model results because the vast majority of shipping noise occurs below 32 kHz. The data were analysed on a multi-processor computing platform using specialised computational tools developed by JASCO. Ambient noise was analysed using Hamming-windowed fast Fourier transforms (FFTs) with 1-Hz resolution and 50% window overlap. A total of 120 FFTs were averaged for each minute of data to yield mean spectra and 1/3-octave band sound pressure levels (SPLs).

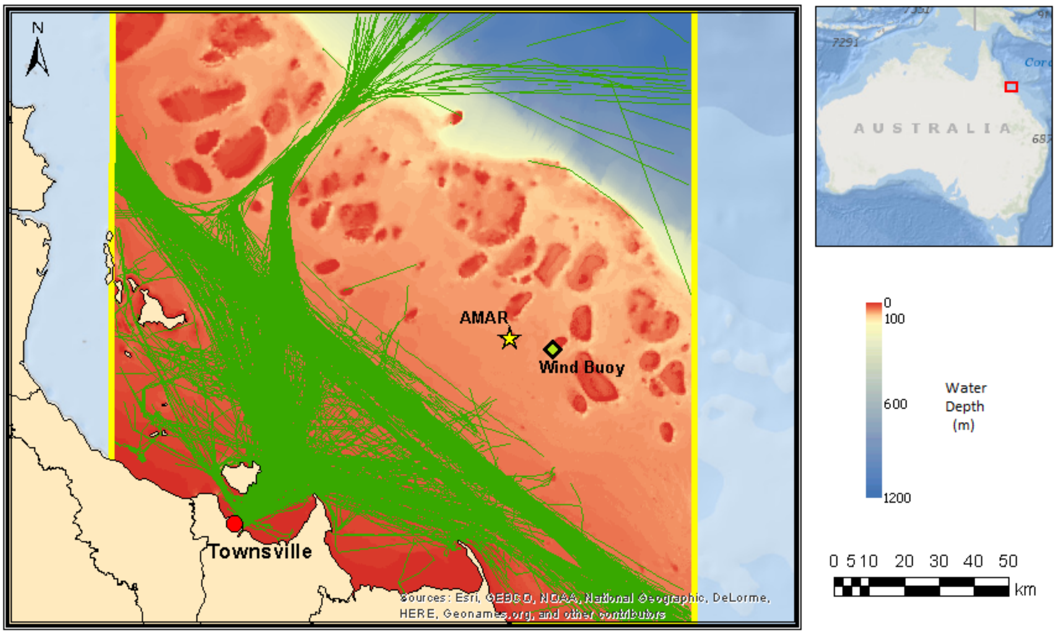

Figure 1 − Map of AIS vessel tracks (green lines) in the study area for Apr–Aug 2013.

2.2 Automated Identification System Data

Shore-based AIS ship tracking data were obtained from MarineTraffic.org for Apr–Aug 2013. Approximately 380,000 vessel position reports were collected inside the study area (Figure 1). Vessels under 300 gross tons are not required to carry AIS transponders, although many small vessels that operate in shipping lanes do so for safety reasons. AIS records included the following vessel information: received time, marine mobile service identity (MMSI), name, latitude, longitude, speed, length overall (LOA), status, heading and type. Erroneous vessel identification accounted for 1% of entries, which were eliminated through manual assessment. Approximately 0.5% of records required consulting online AIS vessel databases to complete the entries for analysis. To analyse the AIS data, the logs were sorted by MMSI and then divided into tracks. Each track represented a contiguous set of position reports from a particular vessel. A new track was assigned to a vessel whenever its AIS transmissions had more than a 1 hour gap, or whenever it moved to or from anchor. We identified 876 unique vessels and 9681 unique tracks in the AIS logs over the three-month period of interest.

2.3 Vessel Source Levels

Modelling the shipping noise emissions of vessels identified in the AIS records meant vessel acoustic source levels had to be estimated. While every vessel has a unique acoustic signature, it is possible to derive representative source spectra for different classes of vessels that are suitable for modelling ship noise over broad spatial and temporal scales (3). For this research, representative source levels for eight different categories of vessels were tabulated. Each vessel in the AIS data was assigned to a category based on its size (LOA), except for tugs, which were categorised separately because their source levels are uncharacteristically high for their size (Table 1). Sailing vessels, search and rescue aircraft, and ships at anchor were present in the AIS data, but were not included in the noise model runs.

Table 1 – Vessel source level categories and modelled source depth.

Category	Description	LOA (m)	Effective Length (m)	Source Depth (m)
1	Vessels by size	> 300	310	6
2	Vessels by size	200-300	253	6
3	Vessels by size	150-200	176	6
4	Vessels by size	100-150	127	6
5	Vessels by size	50-100	78	6
6	Vessels by size	10-50	34	2
7	Vessels by size	< 10	8	2
8	Tugs	-	-	2

Source levels for vessels larger than 50 m LOA (categories 1–5) were based on the merchant ship model of Breeding et al. (4), which estimates source spectral density levels (dB re 1 μPa/√Hz @ 1 m) from ship length and ship speed, according to a power-law model:

$$L_s(f,v,l) = L_{s0}(f) + c_V \times 10\log_{10}(v/v_0) + c_L \times 10\log_{10}(l/l_0) + g(f,l) \quad (1)$$

In this formula, c_V and c_L are power-law coefficients for speed and length (6 and 2, respectively), v_0 is the reference speed, l_0 is the reference length, $L_{s0}(f)$ is a mean reference spectrum, and $g(f,l)$ is an additional length-dependent correction. Source levels for smaller vessels (categories 6–7) were based on averaged measurements from two different studies of small boats, one carried out in Glacier Bay National Park and Preserve, Alaska (5), and the other in the Alaskan Beaufort Sea (6). Source levels for tugs (category 8) were based on averaged measurements from an offshore vessel noise study carried out in the Chukchi Sea, Alaska (7). An effective length was assigned to each size category, based on the weighted average source levels of vessels in each category. Reference source levels for all vessel categories were adjusted to a common reference speed of 10 knots (Figure 2). Time-dependent source levels of vessels in the model were adjusted from the reference source levels according to transit speed, assuming a sixth-power dependence of radiated sound power on ship speed (see Eqn. 1).

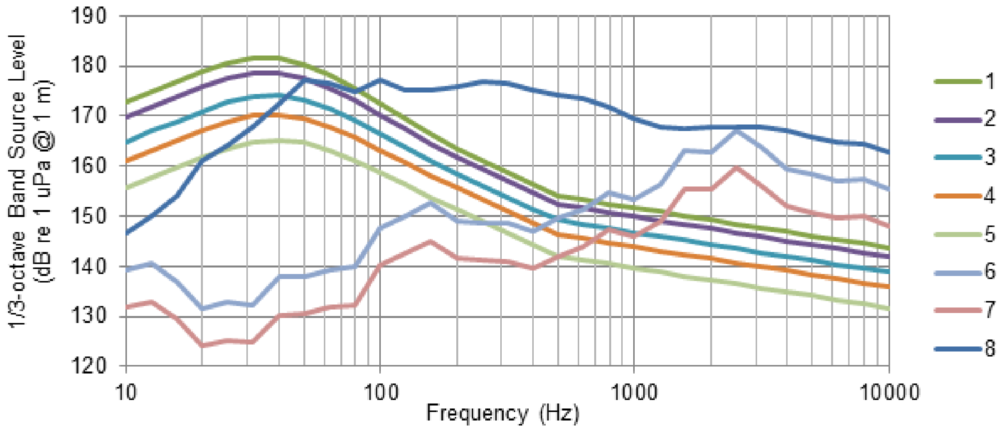

Figure 2 – Source levels by vessel category (1–8) in 1/3-octave frequency bands, adjusted to 10 knot reference speed.

2.4 Model Environmental Parameters

Environmental models of ocean bathymetry, water sound speed profile and seabed geoacoustics were required for modelling transmission loss inside the study area. Bathymetry for the study area was represented on a 100 m resolution UTM grid, based on data obtained from the JCU Deepreef Explorer project (8). Sound speed profiles for the study area were derived from the GDEM ocean temperature and salinity climatology database (9). Temperature and salinity profiles from GDEM were converted to speed of sound in water using standard formulae (10). Because mean GDEM sound speed profiles for Apr–Aug were very similar throughout the study area, a single mean sound speed profile (Figure 3, left) was applied over the period of interest.

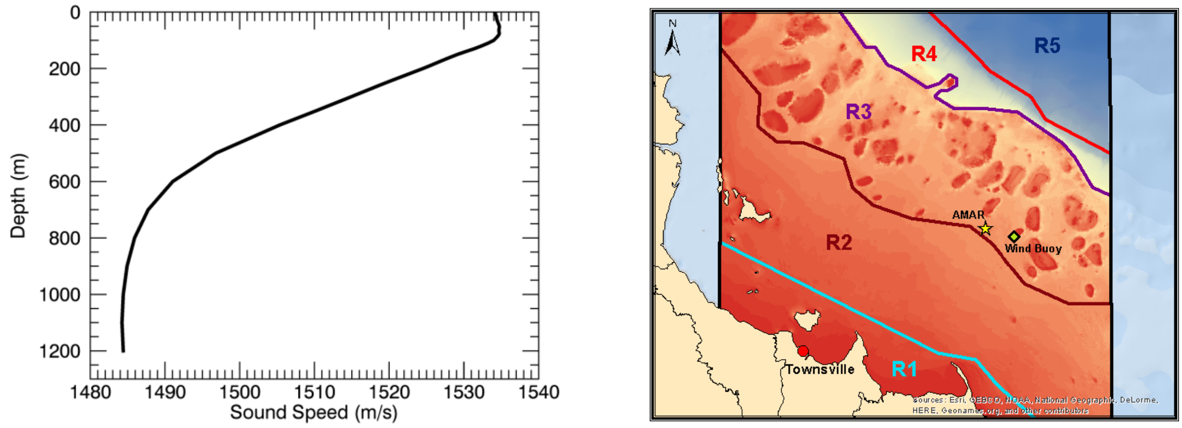

Figure 3 – Left: Average GDEM sound speed profile for the study area for Apr–Aug. Right: Geoacoustic regions used for modelling elasto-acoustic properties of seabed.

Geoacoustic profiles were developed for five different regions inside the study area (Figure 3, right). Published seabed geology data indicate that a thin layer of surficial sediments lies above a limestone substrate over much of the continental shelf in this area (11-13). Surficial sediments are predominantly mud near shore (region 1), transitioning to sand on the shelf (region 2), with exposed limestone in reef areas (region 3) and gravel on the slope (region 4). No seabed geology data were available for deep water (region 5), but data from other locations suggest thin mud over basalt. Elasto-acoustic properties of sediment layers for each region were estimated according to the methods of Hamilton (14) (Table 2).

Table 2 – Geoacoustic properties of seabed layers: h = layer thickness, c_p = P-wave speed, c_s = S-wave speed, α_p = P-wave attenuation, α_s = S-wave attenuation, ρ = density.

	Muddy Sand	Sand	Gravel	Mud	Limestone (basement)	Basalt (basement)
Region	1	2	4	5	1, 2, 3, 4	5
h (m)	5	2.5	2.5	10	∞	∞
c_p (km/s)	1.6	1.7	1.8	1.5	2.9	3.0
c_s (km/s)	0.4	0.425	0.45	0.125	1.35	0.6
α_p (dB/λ)	1.1	1.2	0.9	0.2	0.3	0.02
α_s (dB/λ)	5.3	5.8	6.4	2	0.5	0.07
ρ (g/cm^3)	1.7	1.9	2.0	1.5	2.6	2.7

2.5 Transmission Loss

Transmission loss in the study area was modelled in 1/3-octave bands using the ORCA normal mode model (15). Tables of transmission loss versus range and frequency were calculated for 23 geographic zones, each representing a different combination of water depth and bottom type. Each zone covered one of 11 water depth ranges: 0–5 m, 5–15 m, 15–30 m, 30–45 m, 45–60 m, 60–100 m, 100–250 m, 250–500 m, 500–750 m, 750–1000 m, 1000–1250 m. Normal modes for each zone were computed at 1/3-octave band centre frequencies at the mean water depth. Transmission loss was computed using an incoherent mode sum, which is suitable for representing frequency-averaged sound attenuation in shallow water environments where modes are strongly bottom interacting (10). The transmission loss calculation used a single receiver depth of 14.5 (AMAR depth), or 1 m above the seabed for shallower locations. The tabulated transmission loss values were used to determine sound attenuation with range and frequency for different regions inside the study area (Figure 4).

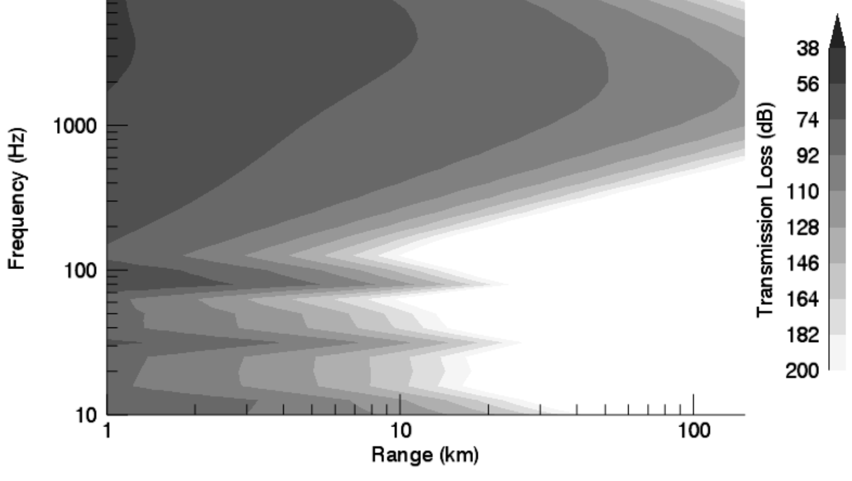

Figure 4 – Sample contour plot of transmission loss versus range and 1/3-octave band frequency for 30–45 m water depth in region 3 (bare limestone), with 2 m source depth.

2.6 Time-dependent Shipping Noise Model

The source level, ship track, and transmission loss data were combined using a specially developed cumulative shipping noise model to estimate time-dependent SPLs inside the study area. SPLs in 1/3-octave bands were modelled on a 150 × 150 km UTM computation grid, where acoustic sources and receivers were assumed to be at the centre of each 1 × 1 km grid cell. For every time increment of the simulation, vessels were assigned to grid cells based on their interpolated coordinates from the track data. For each source cell, a fan of geometric rays was projected to all receiver cells not blocked by land within 150 km range. Along each ray, the 1/3-octave band transmission loss between source and receiver cells was computed from the tabulated transmission loss versus range curves, based on the transmission loss zones traversed by the ray. To accommodate range-dependent transitions between zones, a composite transmission loss curve was created for each ray, based on a recursive sum of the range-dependent transmission loss curve at each range step along the ray:

$$\mathrm{TL}(n\Delta r) = \mathrm{TL}((n-1)\Delta r) + (\mathrm{TL}'[n;k] - \mathrm{TL}'[n-1;k]) \tag{2}$$

In Eqn. 2, Δr is the range increment, n is the range step (an integer), k is the zone number corresponding to step n along the current ray, and $\mathrm{TL}'[n;k]$ denotes the tabulated TL value at step n for zone k. For the special case where the source and receiver cells are identical, TL was calculated by assuming that the radiated sound power in a cell is distributed evenly over the cell's area, resulting in a horizontally uniform sound field. This assumption gives an in-cell TL value of $20\times\log D - 11$, where D is the edge-length of a cell.

The contribution of wind-driven ambient noise was also included in the model. Tabulated curves of 1/3-octave band ambient noise versus frequency and wind speed were obtained from Wenz (16) and Cato (17). Hourly mean wind speed data were obtained from a weather station, operated by the Australian Institute of Marine Science, located on Davies Reef approximately 12 km from the AMAR deployment location. Wind noise SPLs for the study area were interpolated from the Wenz and Cato curves according to the recorded wind speed versus time data from the weather station. Aggregate SPLs in all grid cells were computed from the cumulative sound field of all vessels in the simulation, plus the wind-driven ambient contribution, for each time step in the model. Simulating a single month took approximately 20 hours of computer time on a desktop PC.

The model did not include snapping shrimp or other sources of biological noise. While snapping shrimp are a dominant feature of the soundscape in coastal tropical and sub-tropical environments, their abundance strongly depends on local habitat features (e.g., seabed type, prey abundance), which are challenging to model at large spatial scales (18); therefore, it was not feasible to include them in this research. Snapping shrimp noise is predominantly concentrated at higher frequencies than shipping, so comparing model predictions with data was still possible, but only at lower frequencies.

3. RESULTS

Spatial grids of 1/3-octave band SPLs, covering the entire study area, were computed for each 5-minute interval from 27 Apr to 29 Jul. Broadband SPLs (0.01–11 kHz) were obtained by summing the 1/3-octave band levels. Image plots of the broadband SPL grids were rendered as time-lapse animations, showing the modelled noise field in the study area over three months (Figure 5). Shallow reefs strongly influenced sound propagation in the study area by blocking vessel noise, particularly in the offshore direction.

Broadband SPLs from the model were compared to acoustic data at the AMAR location (Figure 6). The comparison was limited to frequencies below 2250 Hz because snapping shrimp dominated measured sound levels above this frequency. The modelled SPLs followed the overall trend of the AMAR data; however, modelled peak levels from individual vessel passes were generally higher than the corresponding measured peak levels by as much as 10 dB. This indicates that modelled source levels may have been too high for certain types of vessels (mostly merchant ships) or that modelled transmission loss was too low. SPLs were occasionally under predicted during periods when wind speeds were low and no vessels were present. This is attributed to snapping shrimp noise, which limited the lower threshold of measureable background noise at frequencies as low as 200 Hz during otherwise quiet periods.

Octave band probability density functions (PDFs) were computed from the SPL data for all three months and compared to predictions from the model (Figure 7). The modelled SPLs showed good agreement with the data in the mid-frequency range, 100–1000 Hz, but modelled SPLs were systematically higher than the data below 100 Hz, which indicates that the model is over predicting shipping noise at low frequencies. The mismatch at high frequencies was due to snapping shrimp, as discussed previously.

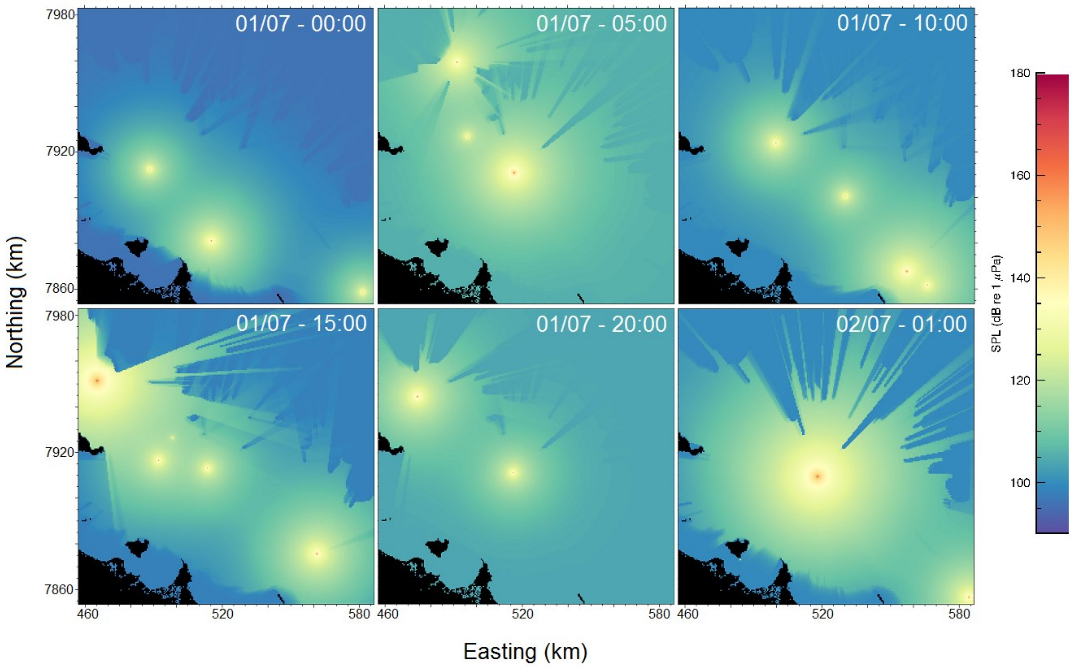

Figure 5 – Sample frames from the time-lapse animation of vessel noise in the study area. Individual frames show broadband SPL (0.09–11 kHz) for 1 Jul 2013 in 5-hour increments.

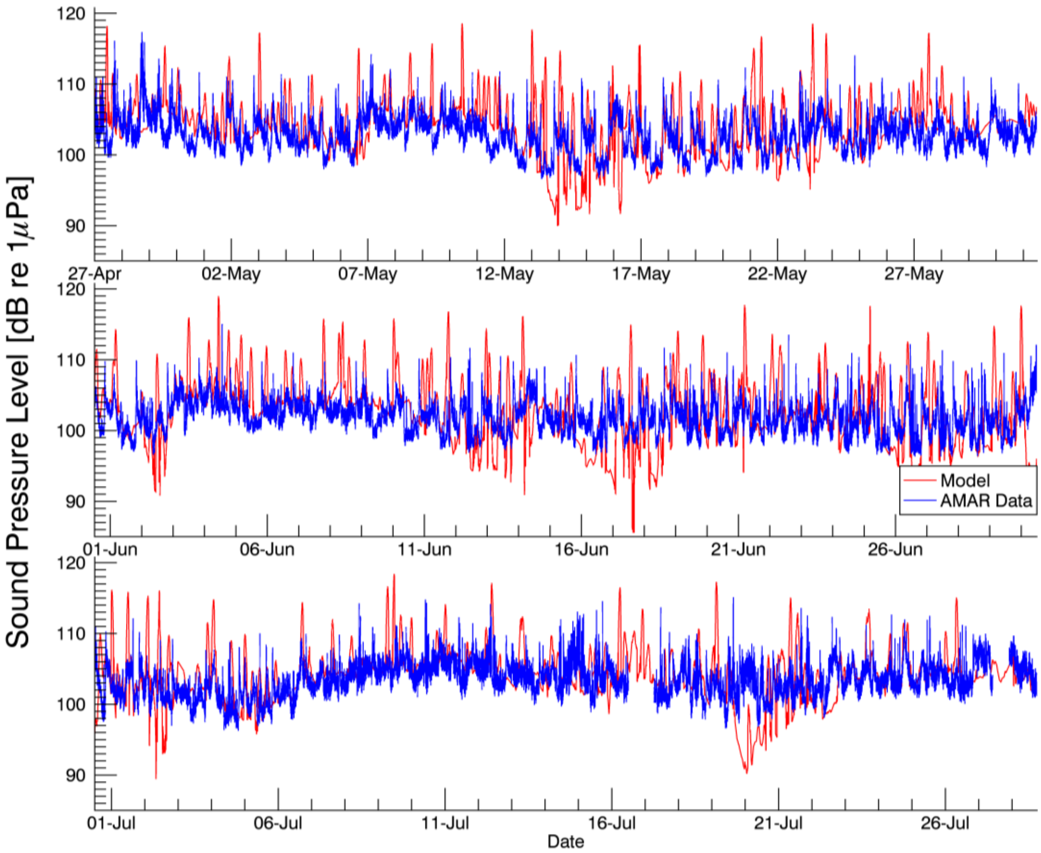

Figure 6 – Comparison of broadband SPLs (0.09–2.25 kHz) computed by the model (red lines) with AMAR data collected at Wheeler Reef (blue lines).

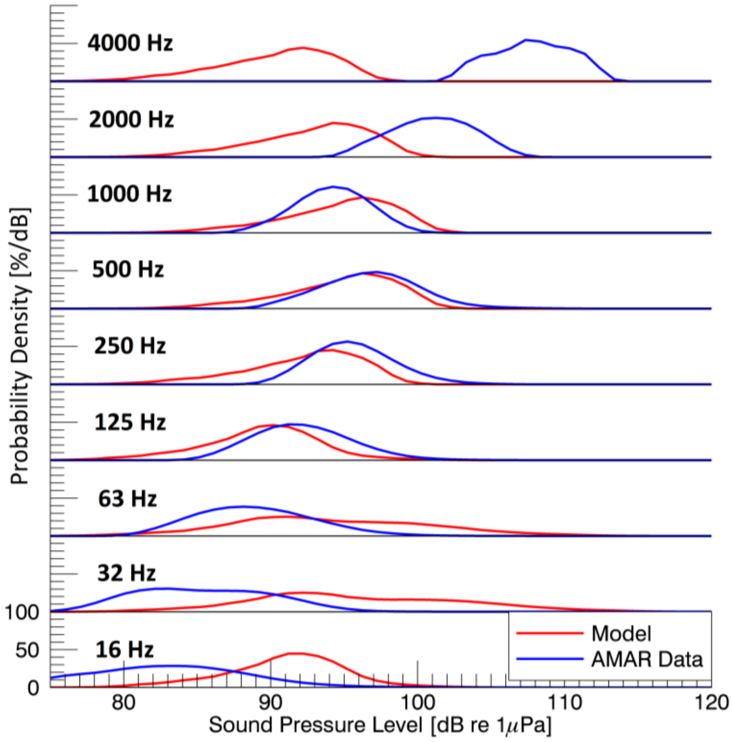

Figure 7 – Comparison of modelled octave band SPL probability density functions (red lines) with AMAR data (blue lines).

4. DISCUSSION AND CONCLUSIONS

Accurate source level estimates are necessary to model shipping noise from large numbers of vessels. Approximately 80% of ships in the study area were large merchant vessels (bulk carriers, tankers, container ships, or vehicle carriers). Results from the current study indicate that the Breeding et al. (4) model may overestimate source levels below 100 Hz for these vessels by 5–10 dB. The accuracy of modelled noise levels could be improved by collecting source level measurements for different classes of vessels in the study area.

Good transmission loss estimates are necessary for modelling shipping noise over large spatial scales, such as those considered in the present study. High-resolution bathymetry and good-quality historical sound speed profile data were available through most of the study area; however, geoacoustic properties of the seabed could only be estimated based on sparsely sampled geological information. Seabed geoacoustic properties strongly influence transmission loss in shallow waters, but the extent to which uncertainties in these properties cause errors in modelled transmission loss is not well understood. A sensitivity analysis that compares modelled transmission loss differences over the range of expected geoacoustic uncertainties could help quantify this effect.

The shore-based AIS data used in the present study also have some limitations. Many smaller boats do not transmit on AIS so they are not included in the sources considered by the model. Source levels of small boats are relatively low, however, so errors introduced by neglecting their contribution are expected to be geographically limited. Furthermore, vessel data transmitted over AIS are not independently verified and occasionally contain errors, although most obvious errors can be corrected by a careful manual review, as was performed during this research. Another feature of AIS is that its coverage is limited by each vessel's VHF radio transmission range, which depends on factors such as transmitter power, transmitter and receiver antenna height and weather conditions. More investigation would be required to estimate the effective AIS coverage within the study area.

Shipping noise levels measured at Wheeler Reef were generally lower than predicted by the model. In principle, the measurements could be used to calibrate the model by analysing data from individual vessel passes to constrain our transmission loss and source levels estimates. In practice, the ships were typically greater than 20 km from the AMAR which is too far away for this purpose. Acoustic measurements collected closer to the main shipping routes are needed to ground truth the model.

Despite these limitations, this research has shown that it is possible to use AIS data with computational acoustic models to efficiently compute cumulative shipping noise levels over large spatial and temporal scales. This is the first anthropogenic propagation modelling study that the authors are aware of in the GBR for anything beyond localised sound sources. The fidelity of the model permits habitat-level assessment of shipping noise effects on marine organisms throughout the study area. Cumulative vessel noise models, like those applied here, can also be used to estimate the relative noise contribution of increased vessel traffic due to future port developments/expansions in restricted and sensitive reef soundscapes and ecosystems. Future research will focus on combining time-dependent noise fields with agent-based (i.e., animat) simulations of animal movement in the study area. Such simulations can be used to statistically analyse noise exposure histories of marine animals in the GBRMP and to estimate potential effects from vessel noise due to aversion, behavioural modifications, and masking.

ACKNOWLEDGEMENTS

The AMAR recording would not have been possible without the assistance of JCU's CSTFA staff, particularly the director, Professor Colin Simpfendorfer, Andrew Tobin and Fernanda de Faria. Their involvement was invaluable, and encompassed all fieldwork-related tasks. Thank you to Katherine Williams from JASCO for technical writing assistance.

REFERENCES

1. Australian Government, Australian Maritime Safety Authority. North-East Shipping Management Plan. 2013. p. 93.
2. Australian Government, Great Barrier Reef Marine Park Authority. Ports and Shipping Information Sheet - Meeting the challenge of an ecologyically sustainable multiple-use marine park. In: Authority GBRMP, editor. Australia: Australian Government; 2013.
3. [NRC] National Research Council. Ocean Noise and Marine Mammals. Washington, DC: National Research Council (U.S.), Ocean Studies Board, Committee on Potential Impacts of Ambient Noise in the Ocean on Marine Mammals. The National Academies Press; 2003.
4. Breeding JE, Pflug LA, Bradley M, Walrod MH, McBride W. Research Ambient Noise Directionality (RANDI) 3.1 Physics Description: Planning System Incorporated1996.
5. Kipple B, Gabriele C. Glacier Bay Watercraft Noise. Prepared by Naval Surface Warfare Center – Carderock Division for Glacier Bay National Park and Preserve, 2003 February 2003. Report No.: Contract No.: NSWCCD-71-TR-2003/522.
6. Zykov M, Hannay D, MacGillivray AO, Austin M, Warner G. Oooguruk Island Acoustic Measurements, 2006: Vessel and Construction Equipment Source Levels. JASCO Report presented to Pioneer Natural Resources Alaska, Inc. and FEX LP, 2008.
7. Austin M, McCrodan A, O'Neill C, Li Z, MacGillivray A. Marine mammal monitoring and mitigation during exploratory drilling by Shell in the Alaskan Chukchi and Beaufort seas, July–November 2012: 90-Day Report. In: Funk DW, Reiser CM, Koski WR, editors. Underwater Sound Measurements: LGL Rep. P1272D–1. Report from LGL Alaska Research Associates Inc., and JASCO Applied Sciences, for Shell Offshore Inc., National Marine Fisheries Service (US), and US Fish and Wildlife Service. 266 pp, plus appendices; 2013.
8. Deepreef Explorer. Bathymetry - Great Barrier Reef and Coral Sea bathymetry 2014 [cited 2014 August 12]. Available from: http://www.deepreef.org/bathymetry/65-3dgbr-bathy.html.
9. Carnes MR. Description and Evaluation of GDEM-V 3.0. US Naval Research Laboratory, Stennis Space Center, MS, 2009 Contract No.: NRL Memorandum Report 7330-09-9165.
10. Jensen FB, Kuperman WA, Porter MB, Schmidt H. Computational Ocean Acoustics. 2nd ed. New York: AIP Press - Springer; 2011. 794 p.
11. Johnson DP, Searle DE. Post-glacial seismic stratigraphy, central Great Barrier Reef, Australia. Sedim. 1984;31:335-52.
12. Mathews E, Heap A, Woods M. Inter-reefal Seabed Sediments and Geomorphology of the Great Barrier Reef: A Spatial Analysis. Spatial Information for the Nation. Canberra, Australia: Australian Government; 2007. p. 140.
13. Bridge T, Done T, Beaman R, Friedman A, Williams S, Pizarro O, et al. Topography, substratum and benthic macrofaunal relationships on a tropical mesophotic shelf margin, central Great Barrier Reef, Australia. Coral Reefs. 2011;30(1):143-53.
14. Hamilton EL. Geoacoustic modeling of the sea floor. J Acoust Soc Am. 1980;68:1313-40.
15. Westwood EK, Tindle CT, Chapman NR. A normal mode model for acousto - elastic ocean environments. J Acoust Soc Am. 1996;100(6):3631-45.
16. Wenz GM. Acoustic ambient noise in the ocean: Spectra and sources. J Acoust Soc Am. 1962 22-Dec-2000;34(12):1936-56. PubMed PMID: 2492.

17. Cato DH. Ocean ambient noise: Its measurement and its significance to marine animals. Proc Inst Acoust. 2008;30(5).

18. Lammers MO, Stieb S, Au WWL, Mooney TA, Brainard RE, Wong K. Temporal, geographic, and density variations in the acoustic activity of snapping shrimp. J Acoust Soc Am. 2006;120(5):3013-.